NON COMPACT EUCLIDEAN CONE 3-MANIFOLDS WITH CONE ANGLES LESS THAN 2π.

DARYL COOPER AND JOAN PORTI

Abstract. We study of noncompact Euclidean cone manifolds with cone angles less than $c < 2\pi$ and singular locus a submanifold. More precisely, we describe its structure outside a compact set. As a corollary we classify those with cone angles $< 2\pi/3$ and those with cone angles $= 2\pi/3$.

1. Introduction

In this paper we study non-compact orientable Euclidean cone 3-manifolds with cone angles less than 2π. When the cone angles are $\leq \pi$ these manifolds are classified: they play a key role in the proof of the orbifold theorem, as they are rescaled limits of collapsing sequences of hyperbolic or spherical cone manifolds [2, 6]. The aim of this paper is to have some understanding when the cone angles lie between π and 2π.

We will fix an *upper bound of the cone angles* $c < 2\pi$. The reason is that if we only impose cone angles $< 2\pi$, the singular locus can have infinitely many components.

For simplicity, we will also restrict to the case where the *singular set is a submanifold.*

The first tool to study those cone manifolds is the soul theorem of Cheeger and Gromoll [5], or its cone manifold version. The soul can have dimension 0, 1 or 2. If the dimension is 1 or 2, then the cone manifold is easy to describe, the difficulties arise when the soul is zero dimensional (i.e. just a point). Notice that the definition of soul is different from the one considered in [2], where it was adapted to cone manifolds with cone angle $\leq \pi$.

The following proposition says that the singular locus is unknotted, provided there are no compact singular components.

Proposition 1.1. *Let E be a Euclidean cone 3-manifold with cone angles $\leq c < 2\pi$ and soul a point. Assume that its singular locus Σ is a non-empty*

2000 *Mathematics Subject Classification.* Primary 57M50; Secondary 53C23.
Key words and phrases. cone manifolds, soul theorem, Alexandrov spaces.

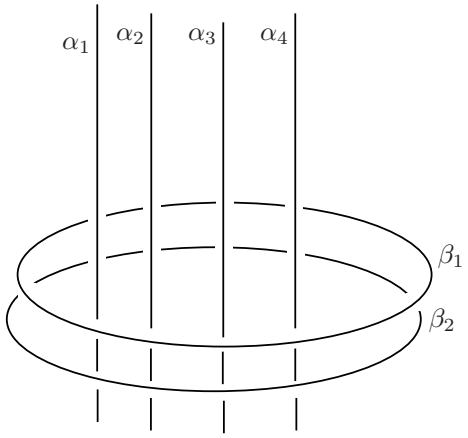

FIGURE 1. The singular locus of a cone manifold as in Example 1.2. The underlying space is $\mathbf{R}^3$, and the angle defects satisfy $\sum(2\pi - \alpha_i) = 2\pi$ and $\sum(2\pi - \beta_i) \leq \pi$.

submanifold. If all components of Σ *are non-compact, then the pair* (E, Σ) *is homeomorphic to* $\mathbf{R}^3$ *with some straight lines.*

When there are compact singular components, we have a nice description away from a compact set. We start with some examples. The *angle defect* of a singularity is 2π minus the cone angle.

Example 1.2. *Consider a Euclidean cone metric on* D^2 *with totally geodesic boundary. Such a metric exists if and only if the sum of the cone angle defects is* 2π*. This metric can be enlarged to a complete metric on the plane by adding a flat cylinder* $S^1 \times [0, \infty)$*, where* $S^1 \times \{0\} = \partial D^2$*. Take the product with* $\mathbf{R}$*, so that we get a three dimensional manifold with closed parallel geodesics. Some of those geodesics can be easily replaced by singular geodesics, provided that the cone angle defects add up to* π*. See Figure 1.*

The topology of the pair (E, Σ) is more involved in the next example, but it can still be described in terms of rational tangles.

Example 1.3. *The product* $[0, 1] \times \mathbf{R}^2$ *is bounded by two parallel planes. Take a geodesic on each plane such that, when parallel transported, they intersect with an angle equal to a rational multiple of* 2π*. Consider the cone manifold obtained by folding these planes along these lines, so that the folding lines become the singular locus, with cone angle* π*. Then, the foliation by segments* $[0, 1] \times \{*\}$ *gives rise to a foliation by geodesic circles, or intervals with end-points in the singular locus. Again, some of the closed*

geodesics can be replaced by singular geodesics with small cone angle defect. The group of transformations in the plane generated by reflections on the two lines is a dihedral group with $2n$ elements, and the sum of the cone angle defects now is bounded above by π/n. See Figure 1.

This example can be further perturbed to replace the edges with cone angle π by several singular edges with cone angle defects whose sum is π.

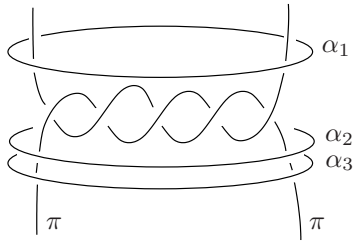

FIGURE 2. The singular locus of a cone manifold as in Example 1.3. $\sum(2\pi - \alpha_i) \leq \frac{\pi}{n}$

Notice that away from a compact set both examples are similar.

Theorem 1.4. *Let E be a non-compact Euclidean cone 3-manifold with cone angles $\leq c < 2\pi$ and such that Σ is a submanifold. Assume that the soul of E is a point and that it has a compact singular component. Then there exists a compact subset K such that:*

(1) either $K = D_1 = D_2$ or $\partial K = D_1 \cup_\partial D_2$, where D_1 and D_2 are totally geodesic discs with geodesic boundary $\partial D_1 = \partial D_2 = D_1 \cap D_2$.
(2) $E - \text{int}(K)$ can be decomposed isometrically in three product pieces: $D_1 \times [0, +\infty)$, $D_2 \times [0, +\infty)$ and $S \times S^1$, where S denotes a Euclidean sector (i.e. its boundary is two half lines) with cone points. The pieces are glued so that $D_i \times [0, \infty) \cap K = D_i \times \{0\}$ and $\partial S \times S^1 = \partial D_1 \times [0, +\infty) \cup_{\partial D_i \times \{0\}} \partial D_2 \times [0, +\infty)$.
(3) The dihedral angle between the discs D_1 and D_2 in ∂K is $\leq \pi$ minus the sum of the angle defects in the sector S.

It can happen that both discs are the same: $K = D_1 = D_2$, as in Example 1.2.

Corollary 1.5. *Let E be a cone manifold as in Theorem 1.4. If the cone angles are $< \frac{3\pi}{2}$, then E is as in Example 1.2.*

Notice that in the case of Example 1.2 the topology of the singular locus is the simplest one. In particular it is the case when cone angles are $< \frac{3\pi}{2}$.

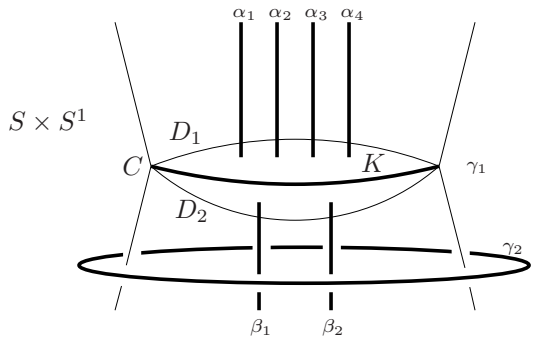

FIGURE 3. Cone manifold as in Theorem 1.4. The interior of K is not described in this picture and the singular locus is represented thicker. The angle defects satisfy $\sum(2\pi-\alpha_i) = \sum(2\pi - \beta_i) = 2\pi$ and $\sum(2\pi - \gamma_i) \leq \pi$

The topology of Example 1.3 is still easy to understand in terms of rational 2-tangles. We shall illustrate in Section 6 that when cone angles are $\frac{3\pi}{2}$ the topology may be more involved. We shall describe cone manifolds with all cone angles precisely equal to $\frac{3\pi}{2}$.

Organization of the paper. In Section 2 we recall the basic properties for Euclidean cone manifolds, including the soul theorem of Cheeger and Gromoll. Section 3 deals with the case of one or two dimensional soul. The zero dimensional case and the proof of Theorem 1.4 is the content of Sections 4 and 5. Finally Section 6 deals with the case where all cone angles equal $\frac{3\pi}{2}$.

Acknowledgements. This research was supported by the Catalan government through grant 2003BEAI400228, the CRM at Barcelona, UCSB and NSF grant DMS-0405963.

2. Euclidean cone manifolds

A *Euclidean cone* 3*-manifold* E is a smooth 3-manifold equipped with a metric so that it is a complete length space locally isometric to

- either the Euclidean space $\mathbf{R}^3$ (smooth points),
- or a neighborhood of a singular edge (singular points).

The local model of the singular points is given, in cylindrical coordinates, by the following metric.

$$ds^2 = dr^2 + \left(\frac{\alpha}{2\pi}r\right)^2 d\theta^2 + dh^2$$

where $r \in (0, +\infty)$ is the distance from the singular axis Σ, $\theta \in [0, 2\pi)$ is the rescaled angle parameter around Σ and $h \in \mathbf{R}$ is the distance along Σ. The angle $\alpha > 0$ is called the *singular angle*. When $\alpha = 2\pi$ this is the standard smooth metric of $\mathbf{R}^3$.

The singular locus will be denoted by Σ and, according to our definition, Σ is a submanifold of codimension two and the cone angle is constant along each connected component. For cone manifolds in general one must allow singular vertices too.

We shall also consider two dimensional cone manifolds; i.e. by taking polar coordinates (r, θ) in the previous description of the singularity, so that the singular locus is discrete.

Remark 2.1. *Since we assume that the cone angles are less than 2π, the cone manifolds considered here are* Alexandrov spaces of non-negative curvature*, hence the corresponding comparison results apply (cf.* [3, 4]*): Toponogov comparison for triangles and hinges, the splitting theorem, etc.*

For instance, using comparison results, in [1, Prop. 8.3] it is proved:

Proposition 2.2. *The number of singular components of a Euclidean cone 3-manifold with cone angles $\leq c < 2\pi$ is finite.*

Soul and Cheeger Gromoll filtration. We briefly recall the construction of Cheeger Gromoll filtration (cf. [5, 2]). Let E be a non-compact Euclidean cone manifold without singular vertices and cone angles $\leq c < 2\pi$. Given a point $p \in E$, we consider all rays $r\colon [0, +\infty) \to E$ starting at p. Since E has non-negative curvature in the Alexandrov sense, Busemann functions $b_r\colon C \to \mathbb{R}$ are convex. For every t, define

$$C_t = \{x \in E \mid b_r(x) \leq t \text{ for all rays } r \text{ starting at } p\}.$$

The sets C_t are convex, give a filtration of E, and if C_{t_2} is not empty then for $t_2 \geq t_1$

$$\partial C_{t_1} = \{x \in C_{t_2} \mid d(x, \partial C_{t_2}) = t_2 - t_1\}.$$

To construct the soul, we start with the smallest t for which C_t is not empty. Then C_t is a convex manifold of dimension less than 3. If this lower dimensional manifold has boundary, we continue to decrease the set by taking distance subsets to the boundary. We stop when we get a submanifold without boundary (possibly a point), which is the soul S.

The sets of this filtration are totally convex, i.e. no geodesic segment with endpoints in this sets can exit them, even if the geodesic is not totally minimizing. The fact that S is totally convex, determines the topology, and even the metric when $\dim S = 2, 1$. Next we discuss the possible dimensions of S.

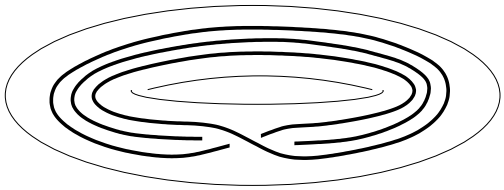

FIGURE 4. Cone manifold with soul S^1.

3. One or two dimensional soul

Let E be a non-compact Euclidean cone 3-manifold with cone angles $\leq c < 2\pi$, and denote by S its soul.

Proposition 3.1. *If* $\dim(S) = 2$*, then* E *is isometric to:*

- *either a product of* $\mathbf{R}$ *with a Euclidean 2-sphere with cone points,*
- *or its orientable quotient, a bundle over the projective plane with cone points.*

On the Euclidean 2-sphere the cone angle defects add up to 4π, and on the projective plane, 2π. In particular, the upper bound $c < 2\pi$ gives an explicit bound on the number of singular components.

Proof: If the soul S is orientable, then E has two ends and, by the splitting theorem, $E = S \times \mathbf{R}$. Since S is a compact Euclidean surface, it must be a sphere with cone points, whose angle defects add up to 4π. If S is non-orientable, then E is the orientable bundle over S, which is a projective plane. By taking the double cover, we reduce to the previous case. □

Proposition 3.2. *If* $\dim(S) = 1$*, then* E *is isometric to the metric suspension of a rotation in a plane with cone points.*

More precisely, E is isometric to $[0,1] \times F^2/\sim$, where F^2 is a plane with singular cone points, and $\sim$ identifies $\{0\} \times F^2$ with $\{1\} \times F^2$ by a rotation (possibly trivial).

Again the cone angle defects on F^2 add up to $< 2\pi$, hence the bound $c < 2\pi$ gives an explicit bound on the number of singular components. If there are singular components other that the suspension of points in F^2 fixed by the rotation, then the rotation has to be of finite order. In this case E is a solid torus and the singular locus is made of fibers of a Seifert fibration with at most one singular fibre.

Proof: Since S is one dimensional, $S \cong S^1$. In particular $\pi_1 E \cong \mathbf{Z}$. In the universal covering, S lifts to a line, hence by the splitting theorem

$\tilde{E} = \mathbf{R} \times F^2$ for F^2 a two dimensional cone manifold. The monodromy of the covering acts on F^2 by isometries, with a fixed point corresponding to the soul.

Notice that F^2 is a non-compact Euclidean cone manifold with non-empty singular locus. Hence the soul of F^2 is a point and F^2 is a plane with several cone points. □

4. Zero dimensional soul

Proposition 4.1. *Let Σ^{noncpt} denote the union of the non-compact components of Σ. If $\dim(S) = 0$, then the pair (E, Σ^{noncpt}) is homeomorphic to $\mathbf{R}^3$ with some straight lines. The sum of the cone angle defects of these non-compact components is $\leq 2\pi$.*

In particular, if Σ has no compact components, the singular locus is unknotted. Notice that again we have an explicit bound of the number of non-compact components of Σ coming from the upper bound on the cone angles $\leq c < 2\pi$.

Proof: Since the soul S is a point, all sets of the Cheeger-Gromoll filtration are balls. Those sets are totally convex, thus they intersect each non-compact geodesic (singular or not) in precisely an interval (possibly empty), even if the geodesic is not minimizing. Furthermore, since the sets of the filtration are strictly convex, if the singular locus meets the boundary of one of these sets then it makes an angle of $\pi/2$ with the boundary. This applies to the non-compact singular components of Σ, therefore, as we increase the sets of the filtration, the singular components intersect the sets in segments that are increasing. This implies the first assertion of the proposition.

For the assertion about the cone angle defects, notice that the sets of the filtration have boundary with non-negative intrinsic curvature, by convexity. The contribution of cone points to the total curvature is larger than the cone angle defects, and we apply Gauss–Bonnet. □

The proof of Theorem 1.4 occupies the remainder of this section and the following one.

Proof of Theorem 1.4: finding the sector $S \times \mathbf{R}$. Let C be a closed singular geodesic in E. By comparison, every ray starting at some point of C must be perpendicular to C. In addition, since the sets of the Cheeger-Gromoll filtration are totally convex, either they contain C or are disjoint from C.

Lemma 4.2. *Every ray starting at C is contained in a flat half-infinite cylinder bounded by C.*

Proof: Consider $r : [0, +\infty) \to E$ a ray with $r(0) \in C$. Toponogov's theorem applied to the triangle with edges C and two copies of $r([0, t])$, when $t \to \infty$, gives that r and C are perpendicular.

Next we show that r can be parallel transported along C by another comparison argument. Consider a parameterized subsegment σ of C starting at $r(0)$ of length x. For $t > 0$, consider also a segment $\bar{\sigma}$ starting at $r(t)$ parallel to σ along r of length x. Let $s = d(\sigma(x), \bar{\sigma}(x))$. We know by comparison that $s \leq t$ and we claim that $s = t$.

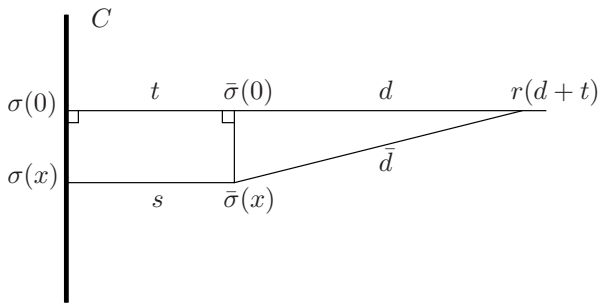

FIGURE 5. Constructing the flat strip

Seeking a contradiction, assume that $s < t$. Choose $d \gg 1$ and set $\bar{d} = d(\bar{\sigma}(x), r(t + d))$. See Figure 4. Since

$$\lim_{d \to +\infty} \sqrt{d^2 + x^2} - d = 0,$$

and $t - s > 0$ by hypothesis, applying comparison d can be chosen large enough so that

$$\bar{d} \leq \sqrt{d^2 + x^2} < d + t - s.$$

Hence $d(r(d + t), C) \leq \bar{d} + s < d + t$. This would imply that C has points inside and outside the sublevel zero set of the Busemann function of r, contradicting total convexity.

This proves that the rays can be parallel transported along C. We claim that this transport does not have monodromy, i.e. once we have made a whole turn around C, the ray is the same, so that it gives a cylinder. We look at the sublevel set 0 for the Busemann function. For any vector v tangent to this sublevel set, the angle between v and r is $\geq \pi/2$. Hence there is no monodromy, otherwise this level set would be two dimensional and C smooth, but we are assuming that the cone angle at C is less than 2π. □

For $p \in C$, all rays starting at p are perpendicular to C, hence the set of rays at p, lies in the set of directions transverse to C, which is a circle of length equal to the cone angle. In addition, those directions form an angle $\geq \pi/2$ with any direction tangent to the subset of the Cheeger-Gromoll filtration. Thus it makes sense to talk about the two extremal or outermost flat strips at C, which are the ones with larger angle.

Lemma 4.3. *The two extremal flat strips at C bound a metric product $S \times S^1$, where S is a 2-dimensional Euclidean sector with cone points and C is the product of S^1 with the tip of the sector.*

Proof: We cut along both extremal flat strips, and consider the connected component with angle $\leq c - \pi < \pi$. We glue the two half planes by an isometry fixing C pointwise. We call Y this new Euclidean cone manifold. The singular geodesic C gives a singular geodesic in Y, that we also denote by C. The new cone angle is the angle between the strips, which is $< \pi$, since it is bounded above by the cone angle of C in E minus π (the angle between any ray and the sets of the Cheeger-Gromoll filtration is $\geq \pi/2$). Since C is a closed singular geodesic in Y with cone angle $< \pi$, it must be contained in the soul of X, because the convex hull of any point close to C meets C (cf. [2, Lemma 4.2.5]). The soul must be C itself, since a two dimensional soul cannot contain a closed singular geodesic. Thus Y is a mapping torus as in Proposition 3.2. The flat strip implies that actually Y is a product, and the lemma is clear. □

5. Asymptotic behavior

In the previous section we found the factor $S \times S^1$. Continuing the proof of Theorem 1.4 and, in order to analyze the rest of the manifold, we remove the interior of the product $S \times S^1$. This space now has two ends, corresponding to the two half-lines in the boundary of the sector S. Let X be one of the ends, i.e. one of the unbounded components if we further remove a convenient compact subset. We will not worry about which compact subset we have removed to analyze X. In order to simplify the argument the proofs below use some standard facts about conemanifolds with boundary. We leave it as an exercise for the reader to check that the proofs can also be done by doubling X along its boundary.

Notice that at each point in $C \subset \partial X$ there is a *single ray* going to ∞, since we have chosen the outermost flat strips. Thus the Tits boundary of X is a single point. The fact that the Tits boundary does not depend on

the base point in X implies that for any two rays in X with $r_1(0) = r_2(0)$,

$$\lim_{t\to+\infty} \frac{d(r_1(t), r_2(t))}{t} = 0.$$

Also, by looking at equivalent definitions (cf. [8]), if $S_R \subset X$ is the metric sphere of radius R centered at some fixed point,

$$\lim_{R\to+\infty} \frac{\operatorname{diam}(S_R)}{R} = 0. \tag{1}$$

Lemma 5.1. *Fix a point $p \in X$. For any $q \in X$, as $d(p,q) \to \infty$, the angle between a minimizing segment to p and a ray starting at q goes to π.*

Proof: Let r be any ray starting at q, and σ any minimizing segment between p and q.

For large t, choose a segment σ' between p and $r(t)$. The segments σ, σ' and a piece of r form a triangle with vertices p, q and $r(t)$. We want to show that its angle at q is close to π. Let q' be the point of σ' such that $d(p,q) = d(p,q')$. By the triangle inequality:

$$|d(q', r(t)) - t| \le d(q, q').$$

Thus

$$|d(p, r(t)) - d(p,q) - t| \le d(q, q').$$

By Equation (1), the ratio $d(q,q')/d(p,q)$ is arbitrarily small, (independently of the choice of t and σ'). By choosing t arbitrarily large, comparison implies that the angle at q between σ and r is arbitrarily close to π. □

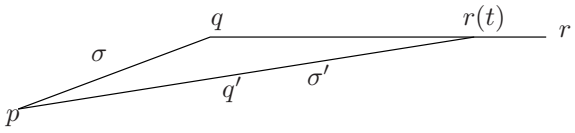

FIGURE 6. The triangle p, q, $r(t)$ in the proof of Lemma 5.1.

Corollary 5.2. *(1) The angle at q between any two minimizing segments to p goes to 0.*
(2) The angle at q between any two rays starting at q goes to 0.
(3) If $q \in \Sigma \cap X$, then the angle between Σ and any minimizing segment to p goes to 0. The angle between Σ and any ray starting at q goes to 0.

Proof: Assertions (1) and (2) are straightforward. To prove (3) we use the upper bound on the cone angle $c < 2\pi$. The directions of σ and r are arbitrarily close to the singular directions, because this is the only way two directions of angle close to π can fit in the space of directions. □

Corollary 5.3. *For any sequence $q_n \to \infty$, the limit of pointed cone manifolds (X, q_n) contains a line.*

Proof: Consider two points at distance d_n from q_n, one on a ray starting at q_n and the other one in a minimizing segment to the base point p. They form a triangle whose angle at q_n goes to π. Choose $d_n \to \infty$ depending on this angle so that the distance between q to the opposite edge of the triangle is bounded. Thus it gives a line at the limit.

Alternatively, Lemma 5.1 implies that the slope of the Busemann function restricted to the segment $\overline{pq}$ goes to one. Hence the union of $\overline{pq}$ with a ray converges to a line. □

It follows from this corollary and the splitting theorem that $\lim(X, q_n) = X_\infty$ is a product. We need however to understand the behavior of the singular locus. We choose q_n so that the distance to the singularity is 1, and q_n is contained in a *parallel copy of C* ie. a smooth closed geodesic parallel to C.

Proposition 5.4. *The limit X_∞ is a cone manifold $X^2 \times \mathbf{R}$. The singular components of the approximates become parallel to give the cone points of X^2, so that when singular components merge at the limit then the cone angle defects add. Moreover X^2 is a disc bounded by a parallel copy of C.*

If the distance between singular components is bounded below away from zero, then X_∞ is a cone manifold and the argument for Proposition 5.4 is easy (see the proof below). Thus, as a preliminary step to prove this proposition, we need to understand how the singularities behave at the limit.

Denote by $\Sigma^1, \dots, \Sigma^k$ the singular components of X. Take x_n^i to be the intersection of Σ^i with the same level set as q_n for the Busemann function. Assume that $d(x_n^1, x_n^2) \to 0$ faster than the other $d(x_n^i, x_n^j)$, i.e. $d(x_n^1, x_n^2) \leq d(x_n^i, x_n^j)$. We take the rescaled limit

$$\lim\left(\frac{1}{d(x_n^1, x_n^2)} X, x_n^1\right) = (X_\infty^1, x_\infty^1).$$

The singular component Σ^1 becomes a line at the limit X_∞^1, because by Lemma 5.1 the slope of the Busemann function on Σ^1 converges to one.

Lemma 5.5. *The injectivity radius in $\frac{1}{d(x_n^1,x_n^2)}X$ at x_n^1 is bounded below away from zero.*

Proof: Consider a small ball centered at x_n^1. It is a metric ball with a singular diameter (which is a piece of Σ^1). Increase its radius until the ball intersect itself or meets a singularity along its boundary; the radius of this ball is the injectivity radius. We control it by finding lower bounds for the length of geodesic paths γ joining x_n^1 to Σ and to the length of geodesic loops l with base point x_n^1.

Let γ be a geodesic path joining x_n^1 to another singular point y_n, so that γ itself is not contained in the singular locus. By taking the shortest one, we may assume that γ is perpendicular to Σ at y_n. By Lemma 5.1 and triangle comparison, γ is almost perpendicular to every ray. Thus the Busemann function restricted to γ is almost constant. Since the Busemann function restricted to the singular components has slope close to one, if $y_n \in \Sigma^1$ then the length of the singular segment $\overline{x_n^1\, y_n} \subset \Sigma^1$ is much shorter than the length $|\gamma|$. When we compute the injectivity radius, we increase the radius of a ball centered at x_n^1, and such a path does not appear. If y_n belongs to some other component Σ^j of Σ, then y_n has to be close to the corresponding x_n^j. Namely, using that the Busemann function b_r restricted to γ has slope less than $\frac{1}{2}$, and restricted to Σ^j more than $\frac{1}{2}$:

$$d(y_n, x_n^j) \leq 2\,|b_r(y_n) - b_r(x_n^j)| = 2\,|b_r(y_n) - b_r(x_n^1)| \leq |\gamma|.$$

Thus

$$|\gamma| \geq d(x_n^1, y_n) \geq d(x_n^1, x_n^j) - d(x_n^j, y_n) \geq 1 - |\gamma|,$$

and $|\gamma| \geq \frac{1}{2}$.

Given a short geodesic loop l with base point x_n^1, by comparison and Lemma 5.1, l is almost perpendicular to Σ^1. Let α be the angle of l at the base point. Since $c < 2\pi$ is the upper bound of the cone angle, almost perpendicularity gives another bound $\alpha \leq c'/2 < \pi$. By pushing l in the direction of the angle at x_n^1, if it does not meet the singular set it shrinks to a point at distance

$$\frac{|l|/2}{\cos(\alpha/2)} \leq \frac{|l|/2}{\cos(c'/2)},$$

where $|l|$ denotes the length of l. So $\frac{|l|/2}{\cos(c'/2)} \geq \frac{1}{2}$, which is the previous bound for $|\gamma|$. This proves the claim. □

Lemma 5.6. *The limit X_∞^1 is a cone manifold.*

Proof of Lemma 5.6: The argument of Lemma 5.5 also gives control of the injectivity radius at each x_n^i. Once the distance to the singular locus is

controlled, the argument with the loops gives an injectivity radius estimate for points in $\frac{1}{d(x_n^1,x_n^2)}X$ at distance at most R from x_n^1, for some fixed $R>0$. This estimate is uniform on n and R. □

Some components Σ^i remain at the limit X_∞^1 (at least Σ^1 and Σ^2), some other components go to infinity. The components that remain at the limit are parallel. We shall use this to prove that, when rescaled by another factor, they converge to a single component whose cone angle defect is the limit.

Proof of Proposition 5.4. We take limits inductively, according to the order of convergence to zero of $d(x_n^i, x_n^j)$, and always taking subsequences, so that we use information from previous steps. More precisely, in the limit X_∞^1 we obtain the singular components Σ^i such that the ratio

$$\frac{d(x_n^1, x_n^i)}{d(x_n^1, x_n^2)}$$

is bounded; the other components go to infinity. We take the pair of coefficients i, j such that $d(x_n^i, x_n^j) \to 0$ with the next order of convergence. If $i, j \neq 1$ and $\frac{d(x_n^1,x_n^j)}{d(x_n^i,x_n^j)} \to \infty$, we repeat the argument of Lemma 5.6 for the base point x_n^j and we do not care about x_n^1. Otherwise we can assume $i = 1$ and take the limit

$$\lim(\frac{1}{d(x_n^1, x_n^j)}X, x_n^j) = (X_\infty^j, x_\infty^j).$$

At the ball $B(x_\infty^j, 1)$ of radius 1, the singularity of the approximating balls $B(x_n^j, 1) \subset \frac{1}{d(x_n^1,x_n^j)}X$ is controlled and therefore $B(x_\infty^j, 1)$ is a cone manifold. By the product structure, X_∞^j is a cone manifold at the neighborhood of Σ^j. The point x_n^1 converges to $x_\infty^1 \in X_\infty^j$ at distance one from x_∞^j. For any $y_\infty \in X_\infty^j$ not in $x_\infty^1 \times \mathbf{R}$, if y_∞ is smooth, then the approximates y_n are at bounded distance from the singularity. Otherwise, if y_∞ is singular, then the y_n are at bounded distance from the other singular components, by the choice of the indices i and j. Thus the arguments in Lemmas 5.5 and 5.6 may be used to say that X_∞^j is locally a cone manifold away from $x_\infty^1 \times \mathbf{R}$.

Claim: $X_\infty^j - (x_\infty^1 \times \mathbf{R})$ is a non-complete product cone manifold.

To take the metric completion of $X_\infty^j - (x_\infty^1 \times \mathbf{R})$, we take an arbitrarily small loop around x_∞^1 . By looking at the approximates to X_∞^1 in Lemma 5.6, hence by changing the base point and the scale factor, the holonomy of this loop must be a rotation of angle 2π minus the sum of angle defects. This follows from the product structure of X_∞^1, and the fact that

the rotation angle of the holonomy does not depend on the scale factor and the choice of the base point (the conjugacy class). Hence the completion is a cone manifold, and the cone angle defect of the singularity is the sum of cone angle defects of singular components merging with Σ^1. This proves the claim.

We iterate this process, which must stop by the finiteness of the number of singular components.

Recall that the base points q_n are contained in parallel copies of C and that the distance to the singular locus is one. Thus the argument of Lemma 5.5 applies to say that the injectivity radius at q_n is bounded below. This implies that the 2-dimensional factor X^2 in the limit is a cone manifold containing at least one cone point and one boundary component which is a geodesic circle. Therefore X^2 must be compact. Notice that the choice of base points q_n does not allow all singularities to merge to a single one, because this would make the length of C go to zero. □

It follows from Proposition 5.4 that the singular components are asymptotically parallel. We claim that they are actually parallel.

Proposition 5.7. *Away from a compact set X is a metric product.*

Proof: By the Cheger-Gromoll filtration, away from a compact set the pair formed by X and its singular locus is topologically a product (Prop. 4.1). By Lemma 5.4, the singular axis at (X, q_n) are almost parallel.

We shall use the direct product structure of the isometry group

$$\mathrm{Isom}^+(\mathbf{R}^3) = \mathbf{R}^3 \rtimes SO(3),$$

and the fact that the holonomy lifts to $\mathbf{R}^3 \rtimes Spin(3)$ [7]. We identify $Spin(3) \cong S^3$ equipped with the standard round metric, so that a rotation in $SO(3)$ of angle $\alpha \in [-\pi, \pi]$ lifts to two points in S^3, which are at respective distance from the identity $|\alpha|/2$ and $\pi - |\alpha|/2$.

The fundamental group of the smooth part $\pi_1(X - \Sigma)$ is a free group generated by the meridians, so we can choose the lifts of their holonomy. In fact we will only look at its projection to $Spin(3)$, that we denote by $A_1, \dots, A_k \in Spin(3)$.

For each meridian (with label i), if α_i is its cone angle defect, we choose A_i so that the distance to the identity in S^3 is $|\alpha_i|/2$. The product of all meridians gives the holonomy of C, which is a pure translation, so the product $A_1 \cdots A_k$ gives either the identity or its antipodal point in S^3, at distance π.

We consider the piecewise geodesic path γ in $Spin(3)$ with ordered vertices Id, A_1, $A_1\,A_2$, …, $A_1\,A_2 \cdots A_k$. Notice that the angles along γ may

depend on the conjugacy classes of the meridians, but not the length of the pieces, because they are precisely half the cone angle defects. By Proposition 5.4, and possibly after reordering the indexes, the conjugacy classes may be chosen so that the angles along the path γ are arbitrarily close to π. Since the length of the pieces of γ are fixed, the endpoint of γ can not be the identity. Thus it is antipodal to the identity. The bound on cone angle defects implies that the length of γ is at most π. Thus it is precisely π and γ is a geodesic, which implies that the singular axis are parallel. □

Conclusion of the Proof of Theorem1.4. Once we know that X is a metric product away from a compact set, we start to decrease the level set of the Busemann function until it meets C. Hence Theorem 1.4 is proved. □

Proof of Corollary 1.5: We apply Theorem 1.4 to E. The dihedral angle between D_1 and D_2 in K is less than the cone angle at C minus π, because any direction in K has an angle $\geq \frac{\pi}{2}$ with any ray, and rays are perpendicular to C. Thus, since the cone angle at C is $\alpha < \frac{3\pi}{2}$, the dihedral angle of the compact K is $< \alpha - \pi < \frac{\pi}{2}$. We claim that this angle is zero. In order to show it, we analyze what happens to the singularity when we shrink K by taking distance subsets. Once the singularity in one of the faces of K reaches this boundary of the face, since the singularity is perpendicular to the face, either it meets immediately the other face (when the angle is zero), or it enters the interior of K (when the angle is larger than $\frac{\pi}{2}$). Since here the dihedral angle is $< \frac{\pi}{2}$, it must be zero. □

In next section we will analyze what happens when the dihedral angle of K is precisely $\frac{\pi}{2}$, which implies working with cone manifolds with cone angle $\frac{3\pi}{2}$. Larger cone angles would probably give more complicated constructions.

6. Constructions from an edge pattern on a parallelepiped

We explain how to construct a non-compact Euclidean cone manifold with cone angles $\frac{3\pi}{2}$ from an edge pattern on a rectangular parallelepiped. Such a cone manifold has soul a point and both closed and unbounded singular geodesics.

A rectangular parallelepiped is a subset of $\mathbf{R}^3$ isometric to the product of three finite closed intervals of positive length. Consider the twelve edges of such a parallelepiped. An *edge pattern* consists of joining the edges into intervals or circles, so that:

(1) The components of the pattern are one or two circles and precisely four intervals.

(2) On each vertex, two of the three edges are joined by the pattern.

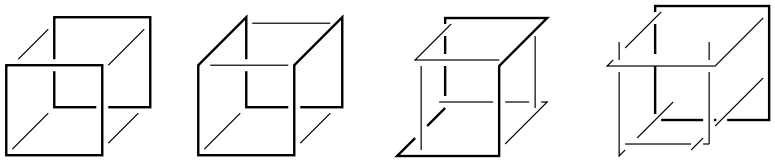

FIGURE 7. Examples of patterns, already realized metrically. The closed components are drawn thicker.

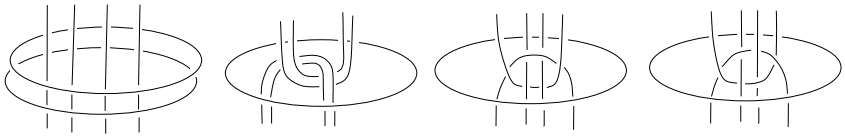

FIGURE 8. The singular locus of the respective cone manifolds of patterns in Figure 7, respecting the order from left to rigth. The underlying space is $\mathbf{R}^3$ and all cone angles $\frac{3}{2}\pi$.

We shall only consider patterns than are metrically realizable in $\mathbf{R}^3$ satisfying the following properties. First we enlarge edges as follows. Those edges which have one free endpoint are enlarged to be unbounded geodesic rays and those with two free endpoints to be complete geodesics. Next we move by parallel transport and slightly shorten those edges which are not part of a circle in the pattern. This must be done so that at each corner the ray in the enlarged edge at that corner lies inside the right angle defined by the other two segments joined in the pattern at that corner. After this is done all the edges must connect up to give the same combinatorial pattern. Notice that this condition for a metric realization already eliminates some patterns, cf. Figure 9.

The cone manifold is constructed as follows. We define a subset in $\mathbf{R}^3$ with piecewise geodesic boundary so that the cone manifold is obtained by gluing its faces. To each (possibly extended) edge I in the metric pattern, remove a *sector* of angle $\frac{\pi}{2}$ from $\mathbf{R}^3$. This sector is a metric subset $I \times S$ bounded by planes parallel to the sides of the parallelepiped. The set S is a sector in the plane orthogonal to I. There are four such sectors and we chose the one which is in the opposite quadrant to the parallelepiped. The condition that the geodesic rays lie inside the right angle defined by

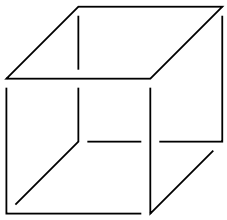

FIGURE 9. Example of pattern that can no be realized metrically in $\mathbf{R}^3$. Notice that the edges must be parellel to coordinate axis.

segments joined in the pattern implies that all the corners of the pattern are removed. The identifications consist of folding each such sector, i.e. in gluing the faces by a rotation. Thus the edges of the pattern give the singular locus.

Definition 6.1. *Such a cone manifold is said to be* constructed from an edge pattern on a parallelepiped.

Notice that two examples on the left of Figure 8 are already described in Examples 1.2 and 1.3, but the two on the right are topologically different.

Theorem 6.2. *Let E be a Euclidean cone manifold with cone angles $\frac{3\pi}{2}$, with soul a point and having a closed singular geodesic. Then E is constructed from an edge pattern in a parallelepiped.*

Proof: We apply Theorem 1.4. Let K be the compact subset, whose boundary is a union of two singular discs along their boundary, which is a singular geodesic C. Since we assume that the cone angle is $\frac{3\pi}{2}$, the dihedral angle of K is at most $\frac{\pi}{2}$. By the same argument as in Corollary 1.5, if the dihedral angle is $< \frac{\pi}{2}$, then E is as in Example 1.2 and therefore it satisfies the theorem. From now on we assume that the dihedral angle is precisely $\frac{\pi}{2}$.

We shrink K by considering K_t supperlevel sets of the distance to ∂K (equivalently the sublevel sets of the Busemann function). Initially, for small t, these subsets are bounded by the union of two faces, forming a dihedral angle along the boundary. Each face is a disc with four cone points. The boundary of K_t stays of this form as it shrinks until a cone point meets the boundary of the disc.

Since we assume that the dihedral angle is $\frac{\pi}{2}$, when a cone point meets the boundary of one of the faces ∂K_t at an edge, a whole segment of the singular component has to lie in the other face of ∂K_t. If we shrink further,

we realize that a new edge on ∂K_t has been created for every pair of cone points going to the boundary of the disc. Now the boundary is a union of flat cone manifolds, meeting along edges with cone angle $\frac{\pi}{2}$, and edges meet at corners, so that each corner is trivalent. If n_{cone} and n_{corner} denote the number of cone points on the faces and corners respectively, then

$$n_{cone} + n_{corner} = 8 \qquad \text{globally on } \partial K_t \tag{2}$$

$$n_{cone} + n_{corner} = 4 \quad \text{on each face of } \partial K_t \tag{3}$$

by the Gauss-Bonnet formula.

We continue the process of shrinking, until some other cone point meets the boundary of the face.

It may happen that a cone point meets the boundary of the face at a corner. By using (3), the corresponding face must be either a triangle with a cone point or a bigon with two cone points. This face cannot have three cone points, because the distance between cone points stays constant during the shrinking, but the face has to collapse. Thus the edges of the corner are different.

When a corner meets a cone point, we change the process of shrinking, so that the speed is not the same on each face. Hence the shrinking process becomes generic and we avoid cone points converging to a corner.

So we assume that the cone points meet the boundary at the interior of an edge. This creates new edges and corners, satisfying Equations (2) and (3), until we end up in one of the following situations:

(a) a smooth point,
(b) a singular point, or
(c) a one or two dimensional cone manifold with boundary.

In case (a), shortly before the collapsing time there are no cone points at all, and formulas (2) and (3) imply that K_t must be combinatorially a cube, hence K_t is isometric to a parallelepiped. In case (b), the same argument gives a triangular prism with two cone points on the upper and lower face. By changing the speed of the faces as before, K_t is non-singular, hence a parallelepiped.

In case (c), some of the faces have collapsed. Since we assume that cone points do not meet corners, the collapsing faces must be rectangles. So shortly before the collapsing time K_t must be a product $X^2 \times [0, \varepsilon]$ or $X^1 \times [0, \varepsilon]^2$, where $\dim X^i = i$. Notice that $X^1 \times [0, \varepsilon]^2$ is already a parallelepiped, and there is nothing to prove. For $X^2 \times [0, \varepsilon]$, the list of all possible X^2 is quickly determined by (3), and it follows that changing the shrinking speed of the faces also gives a parallelepiped. □

References

[1] Michel Boileau, Bernhard Leeb, and Joan Porti. Geometrization of 3-orbifolds. *Ann. of Math. (2)*, 162:195–250, 2005.

[2] Michel Boileau and Joan Porti. Geometrization of 3-orbifolds of cyclic type. *Astérisque*, (272):208, 2001.

[3] Dmitri Burago, Yuri Burago, and Sergei Ivanov. *A course in metric geometry*, volume 33 of *Graduate Studies in Mathematics*. American Mathematical Society, Providence, RI, 2001.

[4] Yu. Burago, M. Gromov, and G. Perel′man. A. D. Aleksandrov spaces with curvatures bounded below. *Uspekhi Mat. Nauk*, 47(2(284)):3–51, 222, 1992.

[5] Jeff Cheeger and Detlef Gromoll. On the structure of complete manifolds of nonnegative curvature. *Ann. of Math. (2)*, 96:413–443, 1972.

[6] Daryl Cooper, Craig D. Hodgson, and Steven P. Kerckhoff. *Three-dimensional orbifolds and cone-manifolds*, volume 5 of *MSJ Memoirs*. Mathematical Society of Japan, Tokyo, 2000. With a postface by Sadayoshi Kojima.

[7] Marc Culler. Lifting representations to covering groups. *Adv. in Math.*, 59(1):64–70, 1986.

[8] Luis Guijarro and Vitali Kapovitch. Restrictions on the geometry at infinity of nonnegatively curved manifolds. *Duke Math. J.*, 78(2):257–276, 1995.

Department of Mathematics, University of California at Santa Barbara, Santa Barbara, CA 93106, USA, cooper@math.ucsb.edu

Departament de Matemàtiques, Universitat Autònoma de Barcelona, E-08193 Bellaterra, Spain, porti@mat.uab.es